



Observation of the decay $B^0 \rightarrow \bar{D}^0 K^+ K^-$ and evidence for $B_s^0 \rightarrow \bar{D}^0 K^+ K^-$

The LHCb collaboration[†]

Abstract

The first observation of the decay $B^0 \rightarrow \bar{D}^0 K^+ K^-$ is reported from an analysis of 0.62 fb^{-1} of pp collision data collected with the LHCb detector. Its branching fraction is measured relative to that of the topologically similar decay $B^0 \rightarrow \bar{D}^0 \pi^+ \pi^-$ to be

$$\frac{\mathcal{B}(B^0 \rightarrow \bar{D}^0 K^+ K^-)}{\mathcal{B}(B^0 \rightarrow \bar{D}^0 \pi^+ \pi^-)} = 0.056 \pm 0.011 \pm 0.007,$$

where the first uncertainty is statistical and the second is systematic. The significance of the signal is 5.8σ . Evidence, with 3.8σ significance, for $B_s^0 \rightarrow \bar{D}^0 K^+ K^-$ decays is also presented. The relative branching fraction is measured to be

$$\frac{\mathcal{B}(B_s^0 \rightarrow \bar{D}^0 K^+ K^-)}{\mathcal{B}(B^0 \rightarrow \bar{D}^0 K^+ K^-)} = 0.90 \pm 0.27 \pm 0.20.$$

These channels are of interest to study the mechanisms behind hadronic B decays, and open new possibilities for CP violation analyses with larger data sets.

Submitted to Phys. Rev. Lett.

[†]Authors are listed on the following pages.

LHCb collaboration

R. Aaij³⁸, C. Abellan Beteta^{33,n}, A. Adametz¹¹, B. Adeva³⁴, M. Adinolfi⁴³, C. Adrover⁶, A. Affolder⁴⁹, Z. Ajaltouni⁵, J. Albrecht³⁵, F. Alessio³⁵, M. Alexander⁴⁸, S. Ali³⁸, G. Alkhazov²⁷, P. Alvarez Cartelle³⁴, A.A. Alves Jr²², S. Amato², Y. Amhis³⁶, L. Anderlini^{17,f}, J. Anderson³⁷, R.B. Appleby⁵¹, O. Aquines Gutierrez¹⁰, F. Archilli^{18,35}, A. Artamonov³², M. Artuso⁵³, E. Aslanides⁶, G. Auriemma^{22,m}, S. Bachmann¹¹, J.J. Back⁴⁵, C. Baesso⁵⁴, V. Balagura²⁸, W. Baldini¹⁶, R.J. Barlow⁵¹, C. Barschel³⁵, S. Barsuk⁷, W. Barter⁴⁴, A. Bates⁴⁸, C. Bauer¹⁰, Th. Bauer³⁸, A. Bay³⁶, J. Beddow⁴⁸, I. Bediaga¹, S. Belogurov²⁸, K. Belous³², I. Belyaev²⁸, E. Ben-Haim⁸, M. Benayoun⁸, G. Bencivenni¹⁸, S. Benson⁴⁷, J. Benton⁴³, A. Berezhnoy²⁹, R. Bernet³⁷, M.-O. Bettler⁴⁴, M. van Beuzekom³⁸, A. Bien¹¹, S. Bifani¹², T. Bird⁵¹, A. Bizzeti^{17,h}, P.M. Björnstad⁵¹, T. Blake³⁵, F. Blanc³⁶, C. Blanks⁵⁰, J. Blouw¹¹, S. Blusk⁵³, A. Bobrov³¹, V. Bocci²², A. Bondar³¹, N. Bondar²⁷, W. Bonivento¹⁵, S. Borghi^{48,51}, A. Borgia⁵³, T.J.V. Bowcock⁴⁹, C. Bozzi¹⁶, T. Brambach⁹, J. van den Brand³⁹, J. Bressieux³⁶, D. Brett⁵¹, M. Britsch¹⁰, T. Britton⁵³, N.H. Brook⁴³, H. Brown⁴⁹, A. Büchler-Germann³⁷, I. Burducea²⁶, A. Bursche³⁷, J. Buytaert³⁵, S. Cadeddu¹⁵, O. Callot⁷, M. Calvi^{20,j}, M. Calvo Gomez^{33,n}, A. Camboni³³, P. Campana^{18,35}, A. Carbone^{14,c}, G. Carboni^{21,k}, R. Cardinale^{19,i,35}, A. Cardini¹⁵, L. Carson⁵⁰, K. Carvalho Akiba², G. Casse⁴⁹, M. Cattaneo³⁵, Ch. Cauet⁹, M. Charles⁵², Ph. Charpentier³⁵, P. Chen^{3,36}, N. Chiapolini³⁷, M. Chrzascz²³, K. Ciba³⁵, X. Cid Vidal³⁴, G. Ciezarek⁵⁰, P.E.L. Clarke⁴⁷, M. Clemencic³⁵, H.V. Cliff⁴⁴, J. Closier³⁵, C. Coca²⁶, V. Coco³⁸, J. Cogan⁶, E. Cogneras⁵, P. Collins³⁵, A. Comerma-Montells³³, A. Contu⁵², A. Cook⁴³, M. Coombes⁴³, G. Corti³⁵, B. Couturier³⁵, G.A. Cowan³⁶, D. Craik⁴⁵, S. Cunliffe⁵⁰, R. Currie⁴⁷, C. D'Ambrosio³⁵, P. David⁸, P.N.Y. David³⁸, I. De Bonis⁴, K. De Bruyn³⁸, S. De Capua^{21,k}, M. De Cian³⁷, J.M. De Miranda¹, L. De Paula², P. De Simone¹⁸, D. Decamp⁴, M. Deckenhoff⁹, H. Degaudenzi^{36,35}, L. Del Buono⁸, C. Deplano¹⁵, D. Derkach^{14,35}, O. Deschamps⁵, F. Dettori³⁹, J. Dickens⁴⁴, H. Dijkstra³⁵, P. Diniz Batista¹, F. Domingo Bonal^{33,n}, S. Donleavy⁴⁹, F. Dordei¹¹, A. Dosil Suárez³⁴, D. Dossett⁴⁵, A. Dovbnya⁴⁰, F. Dupertuis³⁶, R. Dzhelyadin³², A. Dziurda²³, A. Dzyuba²⁷, S. Easo⁴⁶, U. Egede⁵⁰, V. Egorychev²⁸, S. Eidelman³¹, D. van Eijk³⁸, F. Eisele¹¹, S. Eisenhardt⁴⁷, R. Ekelhof⁹, L. Eklund⁴⁸, I. El Rifai⁵, Ch. Elsasser³⁷, D. Elsby⁴², D. Esperante Pereira³⁴, A. Falabella^{14,e}, C. Färber¹¹, G. Fardell⁴⁷, C. Farinelli³⁸, S. Farry¹², V. Fave³⁶, V. Fernandez Albor³⁴, F. Ferreira Rodrigues¹, M. Ferro-Luzzi³⁵, S. Filippov³⁰, C. Fitzpatrick⁴⁷, M. Fontana¹⁰, F. Fontanelli^{19,i}, R. Forty³⁵, O. Francisco², M. Frank³⁵, C. Frei³⁵, M. Frosini^{17,f}, S. Furcas²⁰, A. Gallas Torreira³⁴, D. Galli^{14,c}, M. Gandelman², P. Gandini⁵², Y. Gao³, J.-C. Garnier³⁵, J. Garofoli⁵³, J. Garra Tico⁴⁴, L. Garrido³³, D. Gascon³³, C. Gaspar³⁵, R. Gauld⁵², E. Gersabeck¹¹, M. Gersabeck³⁵, T. Gershon^{45,35}, Ph. Ghez⁴, V. Gibson⁴⁴, V.V. Gligorov³⁵, C. Göbel⁵⁴, D. Golubkov²⁸, A. Golutvin^{50,28,35}, A. Gomes², H. Gordon⁵², M. Grabalosa Gándara³³, R. Graciani Diaz³³, L.A. Granado Cardoso³⁵, E. Graugés³³, G. Graziani¹⁷, A. Greco²⁶, E. Greening⁵², S. Gregson⁴⁴, O. Grünberg⁵⁵, B. Gui⁵³, E. Gushchin³⁰, Yu. Guz³², T. Gys³⁵, C. Hadjivasiliou⁵³, G. Haefeli³⁶, C. Haen³⁵, S.C. Haines⁴⁴, S. Hall⁵⁰, T. Hampson⁴³, S. Hansmann-Menzemer¹¹, N. Harnew⁵², S.T. Harnew⁴³, J. Harrison⁵¹, P.F. Harrison⁴⁵, T. Hartmann⁵⁵, J. He⁷, V. Heijne³⁸, K. Hennessy⁴⁹, P. Henrard⁵, J.A. Hernando Morata³⁴, E. van Herwijnen³⁵, E. Hicks⁴⁹, D. Hill⁵², M. Hoballah⁵, P. Hopchev⁴, W. Hulsbergen³⁸, P. Hunt⁵², T. Huse⁴⁹, N. Hussain⁵², R.S. Huston¹², D. Hutchcroft⁴⁹, D. Hynds⁴⁸, V. Iakovenko⁴¹, P. Ilten¹², J. Imong⁴³,

R. Jacobsson³⁵, A. Jaeger¹¹, M. Jahjah Hussein⁵, E. Jans³⁸, F. Jansen³⁸, P. Jatou³⁶,
 B. Jean-Marie⁷, F. Jing³, M. John⁵², D. Johnson⁵², C.R. Jones⁴⁴, B. Jost³⁵, M. Kabbalo⁹,
 S. Kandybei⁴⁰, M. Karacson³⁵, T.M. Karbach⁹, J. Keaveney¹², I.R. Kenyon⁴², U. Kerzel³⁵,
 T. Ketel³⁹, A. Keune³⁶, B. Khanji²⁰, Y.M. Kim⁴⁷, M. Knecht³⁶, O. Kochebina⁷, I. Komarov²⁹,
 R.F. Koopman³⁹, P. Koppenburg³⁸, M. Korolev²⁹, A. Kozlinskiy³⁸, L. Kravchuk³⁰,
 K. Kreplin¹¹, M. Krepis⁴⁵, G. Krocker¹¹, P. Krokovny³¹, F. Kruse⁹, M. Kucharczyk^{20,23,35,j},
 V. Kudryavtsev³¹, T. Kvaratskheliya^{28,35}, V.N. La Thi³⁶, D. Lacarrere³⁵, G. Lafferty⁵¹,
 A. Lai¹⁵, D. Lambert⁴⁷, R.W. Lambert³⁹, E. Lanciotti³⁵, G. Lanfranchi^{18,35},
 C. Langenbruch³⁵, T. Latham⁴⁵, C. Lazzeroni⁴², R. Le Gac⁶, J. van Leerdam³⁸, J.-P. Lees⁴,
 R. Lefèvre⁵, A. Leflat^{29,35}, J. Lefrançois⁷, O. Leroy⁶, T. Lesiak²³, L. Li³, Y. Li³, L. Li Gioi⁵,
 M. Lieng⁹, M. Liles⁴⁹, R. Lindner³⁵, C. Linn¹¹, B. Liu³, G. Liu³⁵, J. von Loeben²⁰,
 J.H. Lopes², E. Lopez Asamar³³, N. Lopez-March³⁶, H. Lu³, J. Luisier³⁶, A. Mac Raighne⁴⁸,
 F. Machefert⁷, I.V. Machikhiliyan^{4,28}, F. Maciuc¹⁰, O. Maev^{27,35}, J. Magnin¹, S. Malde⁵²,
 R.M.D. Mamunur³⁵, G. Manca^{15,d}, G. Mancinelli⁶, N. Mangiafave⁴⁴, U. Marconi¹⁴,
 R. Märki³⁶, J. Marks¹¹, G. Martellotti²², A. Martens⁸, L. Martin⁵², A. Martín Sánchez⁷,
 M. Martinelli³⁸, D. Martinez Santos³⁵, A. Massafferri¹, Z. Mathe¹², C. Matteuzzi²⁰,
 M. Matveev²⁷, E. Maurice⁶, A. Mazurov^{16,30,35}, J. McCarthy⁴², G. McGregor⁵¹, R. McNulty¹²,
 M. Meissner¹¹, M. Merk³⁸, J. Merkel⁹, D.A. Milanes¹³, M.-N. Minard⁴, J. Molina Rodriguez⁵⁴,
 S. Monteil⁵, D. Moran⁵¹, P. Morawski²³, R. Mountain⁵³, I. Mous³⁸, F. Muheim⁴⁷, K. Müller³⁷,
 R. Muresan²⁶, B. Muryn²⁴, B. Muster³⁶, J. Mylroie-Smith⁴⁹, P. Naik⁴³, T. Nakada³⁶,
 R. Nandakumar⁴⁶, I. Nasteva¹, M. Needham⁴⁷, N. Neufeld³⁵, A.D. Nguyen³⁶,
 C. Nguyen-Mau^{36,o}, M. Nicol⁷, V. Niess⁵, N. Nikitin²⁹, T. Nikodem¹¹, A. Nomerotski^{52,35},
 A. Novoselov³², A. Oblakowska-Mucha²⁴, V. Obraztsov³², S. Oggero³⁸, S. Ogilvy⁴⁸,
 O. Okhrimenko⁴¹, R. Oldeman^{15,d,35}, M. Orlandea²⁶, J.M. Otalora Goicochea², P. Owen⁵⁰,
 B.K. Pal⁵³, A. Palano^{13,b}, M. Palutan¹⁸, J. Panman³⁵, A. Papanestis⁴⁶, M. Pappagallo⁴⁸,
 C. Parkes⁵¹, C.J. Parkinson⁵⁰, G. Passaleva¹⁷, G.D. Patel⁴⁹, M. Patel⁵⁰, G.N. Patrick⁴⁶,
 C. Patrignani^{19,i}, C. Pavel-Nicorescu²⁶, A. Pazos Alvarez³⁴, A. Pellegrino³⁸, G. Penso^{22,l},
 M. Pepe Altarelli³⁵, S. Perazzini^{14,c}, D.L. Perego^{20,j}, E. Perez Trigo³⁴,
 A. Pérez-Calero Yzquierdo³³, P. Perret⁵, M. Perrin-Terrin⁶, G. Pessina²⁰, A. Petrolini^{19,i},
 A. Phan⁵³, E. Picatoste Olloqui³³, B. Pie Valls³³, B. Pietrzyk⁴, T. Pilař⁴⁵, D. Pinci²²,
 S. Playfer⁴⁷, M. Plo Casasus³⁴, F. Polci⁸, G. Polok²³, A. Poluektov^{45,31}, E. Polcarpo²,
 D. Popov¹⁰, B. Popovici²⁶, C. Potterat³³, A. Powell⁵², J. Prisciandaro³⁶, V. Pugatch⁴¹,
 A. Puig Navarro³³, W. Qian³, J.H. Rademacker⁴³, B. Rakotomiamanana³⁶, M.S. Rangel²,
 I. Raniuk⁴⁰, N. Rauschmayr³⁵, G. Raven³⁹, S. Redford⁵², M.M. Reid⁴⁵, A.C. dos Reis¹,
 S. Ricciardi⁴⁶, A. Richards⁵⁰, K. Rinnert⁴⁹, D.A. Roa Romero⁵, P. Robbe⁷, E. Rodrigues^{48,51},
 P. Rodriguez Perez³⁴, G.J. Rogers⁴⁴, S. Roiser³⁵, V. Romanovsky³², A. Romero Vidal³⁴,
 M. Rosello^{33,n}, J. Rouvinet³⁶, T. Ruf³⁵, H. Ruiz³³, G. Sabatino^{21,k}, J.J. Saborido Silva³⁴,
 N. Sagidova²⁷, P. Sail⁴⁸, B. Saitta^{15,d}, C. Salzmann³⁷, B. Sanmartin Sedes³⁴, M. Sannino^{19,i},
 R. Santacesaria²², C. Santamarina Rios³⁴, R. Santinelli³⁵, E. Santovetti^{21,k}, M. Sapunov⁶,
 A. Sarti^{18,l}, C. Satriano^{22,m}, A. Satta²¹, M. Savrie^{16,e}, D. Savrina²⁸, P. Schaack⁵⁰,
 M. Schiller³⁹, H. Schindler³⁵, S. Schleich⁹, M. Schlupp⁹, M. Schmelling¹⁰, B. Schmidt³⁵,
 O. Schneider³⁶, A. Schopper³⁵, M.-H. Schune⁷, R. Schwemmer³⁵, B. Sciascia¹⁸, A. Sciubba^{18,l},
 M. Seco³⁴, A. Semennikov²⁸, K. Senderowska²⁴, I. Sepp⁵⁰, N. Serra³⁷, J. Serrano⁶, P. Seyfert¹¹,
 M. Shapkin³², I. Shapoval^{40,35}, P. Shatalov²⁸, Y. Shcheglov²⁷, T. Shears⁴⁹, L. Shekhtman³¹,
 O. Shevchenko⁴⁰, V. Shevchenko²⁸, A. Shires⁵⁰, R. Silva Coutinho⁴⁵, T. Skwarnicki⁵³,
 N.A. Smith⁴⁹, E. Smith^{52,46}, M. Smith⁵¹, K. Sobczak⁵, F.J.P. Soler⁴⁸, A. Solomin⁴³,

F. Soomro^{18,35}, D. Souza⁴³, B. Souza De Paula², B. Spaan⁹, A. Sparkes⁴⁷, P. Spradlin⁴⁸, F. Stagni³⁵, S. Stahl¹¹, O. Steinkamp³⁷, S. Stoica²⁶, S. Stone⁵³, B. Storaci³⁸, M. Straticiu²⁶, U. Straumann³⁷, V.K. Subbiah³⁵, S. Swientek⁹, M. Szczekowski²⁵, P. Szczypka^{36,35}, T. Szumlak²⁴, S. T'Jampens⁴, M. Teklishyn⁷, E. Teodorescu²⁶, F. Teubert³⁵, C. Thomas⁵², E. Thomas³⁵, J. van Tilburg¹¹, V. Tisserand⁴, M. Tobin³⁷, S. Tol³⁹, S. Topp-Joergensen⁵², N. Torr⁵², E. Tournefier^{4,50}, S. Tourneur³⁶, M.T. Tran³⁶, A. Tsaregorodtsev⁶, N. Tuning³⁸, M. Ubeda Garcia³⁵, A. Ukleja²⁵, U. Uwer¹¹, V. Vagnoni¹⁴, G. Valenti¹⁴, R. Vazquez Gomez³³, P. Vazquez Regueiro³⁴, S. Vecchi¹⁶, J.J. Velthuis⁴³, M. Veltri^{17,g}, G. Veneziano³⁶, M. Vesterinen³⁵, B. Viaud⁷, I. Videau⁷, D. Vieira², X. Vilasis-Cardona^{33,n}, J. Visniakov³⁴, A. Vollhardt³⁷, D. Volyanskyy¹⁰, D. Voong⁴³, A. Vorobyev²⁷, V. Vorobyev³¹, C. Voß⁵⁵, H. Voss¹⁰, R. Waldi⁵⁵, R. Wallace¹², S. Wandernoth¹¹, J. Wang⁵³, D.R. Ward⁴⁴, N.K. Watson⁴², A.D. Webber⁵¹, D. Websdale⁵⁰, M. Whitehead⁴⁵, J. Wicht³⁵, D. Wiedner¹¹, L. Wiggers³⁸, G. Wilkinson⁵², M.P. Williams^{45,46}, M. Williams⁵⁰, F.F. Wilson⁴⁶, J. Wishahi⁹, M. Witek²³, W. Witzeling³⁵, S.A. Wotton⁴⁴, S. Wright⁴⁴, S. Wu³, K. Wyllie³⁵, Y. Xie⁴⁷, F. Xing⁵², Z. Xing⁵³, Z. Yang³, R. Young⁴⁷, X. Yuan³, O. Yushchenko³², M. Zangoli¹⁴, M. Zavertyaev^{10,a}, F. Zhang³, L. Zhang⁵³, W.C. Zhang¹², Y. Zhang³, A. Zhelezov¹¹, L. Zhong³, A. Zvyagin³⁵.

¹ *Centro Brasileiro de Pesquisas Físicas (CBPF), Rio de Janeiro, Brazil*

² *Universidade Federal do Rio de Janeiro (UFRJ), Rio de Janeiro, Brazil*

³ *Center for High Energy Physics, Tsinghua University, Beijing, China*

⁴ *LAPP, Université de Savoie, CNRS/IN2P3, Annecy-Le-Vieux, France*

⁵ *Clermont Université, Université Blaise Pascal, CNRS/IN2P3, LPC, Clermont-Ferrand, France*

⁶ *CPPM, Aix-Marseille Université, CNRS/IN2P3, Marseille, France*

⁷ *LAL, Université Paris-Sud, CNRS/IN2P3, Orsay, France*

⁸ *LPNHE, Université Pierre et Marie Curie, Université Paris Diderot, CNRS/IN2P3, Paris, France*

⁹ *Fakultät Physik, Technische Universität Dortmund, Dortmund, Germany*

¹⁰ *Max-Planck-Institut für Kernphysik (MPIK), Heidelberg, Germany*

¹¹ *Physikalisches Institut, Ruprecht-Karls-Universität Heidelberg, Heidelberg, Germany*

¹² *School of Physics, University College Dublin, Dublin, Ireland*

¹³ *Sezione INFN di Bari, Bari, Italy*

¹⁴ *Sezione INFN di Bologna, Bologna, Italy*

¹⁵ *Sezione INFN di Cagliari, Cagliari, Italy*

¹⁶ *Sezione INFN di Ferrara, Ferrara, Italy*

¹⁷ *Sezione INFN di Firenze, Firenze, Italy*

¹⁸ *Laboratori Nazionali dell'INFN di Frascati, Frascati, Italy*

¹⁹ *Sezione INFN di Genova, Genova, Italy*

²⁰ *Sezione INFN di Milano Bicocca, Milano, Italy*

²¹ *Sezione INFN di Roma Tor Vergata, Roma, Italy*

²² *Sezione INFN di Roma La Sapienza, Roma, Italy*

²³ *Henryk Niewodniczanski Institute of Nuclear Physics Polish Academy of Sciences, Kraków, Poland*

²⁴ *AGH University of Science and Technology, Kraków, Poland*

²⁵ *Soltan Institute for Nuclear Studies, Warsaw, Poland*

²⁶ *Horia Hulubei National Institute of Physics and Nuclear Engineering, Bucharest-Magurele, Romania*

²⁷ *Petersburg Nuclear Physics Institute (PNPI), Gatchina, Russia*

²⁸ *Institute of Theoretical and Experimental Physics (ITEP), Moscow, Russia*

²⁹ *Institute of Nuclear Physics, Moscow State University (SINP MSU), Moscow, Russia*

³⁰ *Institute for Nuclear Research of the Russian Academy of Sciences (INR RAN), Moscow, Russia*

³¹ *Budker Institute of Nuclear Physics (SB RAS) and Novosibirsk State University, Novosibirsk, Russia*

³² *Institute for High Energy Physics (IHEP), Protvino, Russia*

- ³³ *Universitat de Barcelona, Barcelona, Spain*
- ³⁴ *Universidad de Santiago de Compostela, Santiago de Compostela, Spain*
- ³⁵ *European Organization for Nuclear Research (CERN), Geneva, Switzerland*
- ³⁶ *Ecole Polytechnique Fédérale de Lausanne (EPFL), Lausanne, Switzerland*
- ³⁷ *Physik-Institut, Universität Zürich, Zürich, Switzerland*
- ³⁸ *Nikhef National Institute for Subatomic Physics, Amsterdam, The Netherlands*
- ³⁹ *Nikhef National Institute for Subatomic Physics and VU University Amsterdam, Amsterdam, The Netherlands*
- ⁴⁰ *NSC Kharkiv Institute of Physics and Technology (NSC KIPT), Kharkiv, Ukraine*
- ⁴¹ *Institute for Nuclear Research of the National Academy of Sciences (KINR), Kyiv, Ukraine*
- ⁴² *University of Birmingham, Birmingham, United Kingdom*
- ⁴³ *H.H. Wills Physics Laboratory, University of Bristol, Bristol, United Kingdom*
- ⁴⁴ *Cavendish Laboratory, University of Cambridge, Cambridge, United Kingdom*
- ⁴⁵ *Department of Physics, University of Warwick, Coventry, United Kingdom*
- ⁴⁶ *STFC Rutherford Appleton Laboratory, Didcot, United Kingdom*
- ⁴⁷ *School of Physics and Astronomy, University of Edinburgh, Edinburgh, United Kingdom*
- ⁴⁸ *School of Physics and Astronomy, University of Glasgow, Glasgow, United Kingdom*
- ⁴⁹ *Oliver Lodge Laboratory, University of Liverpool, Liverpool, United Kingdom*
- ⁵⁰ *Imperial College London, London, United Kingdom*
- ⁵¹ *School of Physics and Astronomy, University of Manchester, Manchester, United Kingdom*
- ⁵² *Department of Physics, University of Oxford, Oxford, United Kingdom*
- ⁵³ *Syracuse University, Syracuse, NY, United States*
- ⁵⁴ *Pontifícia Universidade Católica do Rio de Janeiro (PUC-Rio), Rio de Janeiro, Brazil, associated to ²*
- ⁵⁵ *Institut für Physik, Universität Rostock, Rostock, Germany, associated to ¹¹*

^a *P.N. Lebedev Physical Institute, Russian Academy of Science (LPI RAS), Moscow, Russia*

^b *Università di Bari, Bari, Italy*

^c *Università di Bologna, Bologna, Italy*

^d *Università di Cagliari, Cagliari, Italy*

^e *Università di Ferrara, Ferrara, Italy*

^f *Università di Firenze, Firenze, Italy*

^g *Università di Urbino, Urbino, Italy*

^h *Università di Modena e Reggio Emilia, Modena, Italy*

ⁱ *Università di Genova, Genova, Italy*

^j *Università di Milano Bicocca, Milano, Italy*

^k *Università di Roma Tor Vergata, Roma, Italy*

^l *Università di Roma La Sapienza, Roma, Italy*

^m *Università della Basilicata, Potenza, Italy*

ⁿ *LIFAEELS, La Salle, Universitat Ramon Llull, Barcelona, Spain*

^o *Hanoi University of Science, Hanoi, Viet Nam*

The precise measurement of the angle γ of the CKM Unitarity Triangle [1, 2] is one of the primary objectives of flavour physics experiments. Prior to the start of LHC data-taking, the combination of measurements with the decay mode $B^+ \rightarrow DK^+$, where D denotes a neutral charmed meson that is an admixture of D^0 and \bar{D}^0 , gave a constraint on γ with an uncertainty of around 20° [3]. Recent results from LHCb on $B^+ \rightarrow DK^+$ [4] have helped to reduce this uncertainty, but the use of additional channels to improve further the precision is of great interest. The as-yet unobserved decay $B_s^0 \rightarrow D\phi$ is one of the modes with potential to make a significant impact on the overall determination of γ [5–7]. Moreover, a Dalitz plot analysis of $B_s^0 \rightarrow DK^+K^-$ can further improve the sensitivity to γ due to heightened sensitivity to interference effects, as well as allowing a determination of ϕ_s , the CP -violating phase in the $B_s^0-\bar{B}_s^0$ system, with minimal theoretical uncertainties [8].

The first step in the programme towards the measurement of γ using the $B_s^0 \rightarrow DK^+K^-$ decay is the observation of the channel. In this Letter the results of a search for neutral B meson decays to $\bar{D}^0K^+K^-$ are presented. The quantities measured include small contributions from decays to $D^0K^+K^-$. The inclusion of charge conjugate modes is implied throughout.

The analysis uses 0.62 fb^{-1} of LHC collision data at a centre-of-mass energy of 7 TeV collected with the LHCb detector during 2011. In high energy pp collisions all b hadron species are produced, so both B^0 and B_s^0 decays are searched for simultaneously. The decay $B^0 \rightarrow \bar{D}^0K^+K^-$ can be mediated by the decay diagrams shown in Fig. 1. These are a W -exchange diagram similar to that for the decay $B^0 \rightarrow D_s^-K^+$ [9, 10] (in this case an excited state that decays to \bar{D}^0K^- , such as D_{s2}^{*-} (2573), would be produced), and a colour-suppressed tree diagram producing \bar{D}^0h^0 , where h^0 is a light unflavoured meson such as $a_0(980)$ that subsequently decays to K^+K^- . Related B decays with $s\bar{s}$ production, $B^+ \rightarrow \bar{D}^0K^+K^{(*)0}$ [11] and $B^+ \rightarrow D_s^{(*)-}K^+\pi^+$ [12, 13], have been measured to have branching fractions of $\mathcal{O}(10^{-4})$.

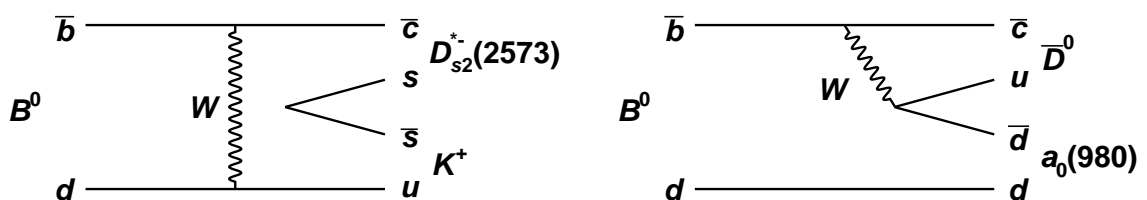


Figure 1: Sample decay diagrams that contribute to the $B^0 \rightarrow \bar{D}^0K^+K^-$ final state via (left) W -exchange, (right) rescattering from a colour-suppressed decay.

The LHCb detector [14] is a single-arm forward spectrometer covering the pseudorapidity range $2 < \eta < 5$, designed for the study of particles containing b or c quarks. The detector includes a high precision tracking system consisting of a silicon-strip vertex detector surrounding the pp interaction region, a large-area silicon-strip detector

located upstream of a dipole magnet with a bending power of about 4 Tm, and three stations of silicon-strip detectors and straw drift tubes placed downstream. The combined tracking system has momentum resolution $\Delta p/p$ that varies from 0.4% at 5 GeV/c to 0.6% at 100 GeV/c, and impact parameter (IP) resolution of 20 μm for tracks with high transverse momentum (p_{T}). Charged hadrons are identified using two ring-imaging Cherenkov (RICH) detectors. Photon, electron and hadron candidates are identified by a calorimeter system consisting of scintillating-pad and pre-shower detectors, an electromagnetic calorimeter and a hadronic calorimeter. Muons are identified by a system composed of alternating layers of iron and multiwire proportional chambers. The trigger consists of a hardware stage, based on information from the calorimeter and muon systems, followed by a software stage which applies a full event reconstruction. In this analysis, signal candidates are accepted if one of the final state particles created a cluster in the calorimeter with sufficient transverse energy to fire the hardware trigger. Events that are triggered at hardware level by the decay products of the other b hadron in the $pp \rightarrow b\bar{b}X$ event are also retained.

The software trigger requires characteristic signatures of b hadron decays: at least one track, with high p_{T} and a large IP with respect to any primary interaction vertex (PV) [15], that subsequently forms part of a two-, three- or four-track secondary vertex with a high sum of the p_{T} of the tracks and significant displacement from the PV [16]. In the offline analysis, the software trigger decision is required to be due to the candidate signal decay.

Candidates that are consistent with the decay chain $B_{(s)}^0 \rightarrow \bar{D}^0 K^+ K^-$, $\bar{D}^0 \rightarrow K^+ \pi^-$ are selected. In order to reduce systematic uncertainties in the measurement, the topologically similar decay $\bar{D}^0 \pi^+ \pi^-$, which has previously been well studied [17, 18], is used as a normalisation channel. The \bar{D}^0 candidate invariant mass is required to satisfy $1844 < m_{K\pi} < 1884 \text{ MeV}/c^2$. Tracks are required to be consistent with either the kaon or pion hypothesis, as appropriate, based on particle identification (PID) information from the RICH detectors. All other selection criteria were tuned on the $\bar{D}^0 \pi^+ \pi^-$ channel. The large yields available in the normalisation sample allow the selection to be based on data, though the efficiencies are determined using Monte Carlo (MC) simulated events. For the simulation, pp collisions are generated using PYTHIA 6.4 [19] with a specific LHCb configuration [20]. Decays of hadronic particles are described by EVTGEN [21]. The interaction of the generated particles with the detector and its response are implemented using the GEANT4 toolkit [22] as described in Ref. [23].

Selection requirements are applied to obtain a clear signal peak in the $\bar{D}^0 \pi^+ \pi^-$ normalisation channel. The selection includes criteria on the track quality of the tracks forming the signal candidate, their p , p_{T} and inconsistency with originating from the PV (χ_{IP}^2). Requirements are also placed on the corresponding variables for candidate composite particles (\bar{D}^0 , $B_{(s)}^0$) together with restrictions on the consistency of the decay fit (χ_{vertex}^2), the flight distance significance (χ_{flight}^2), and the angle between the momentum vector and the line joining the PV to the $B_{(s)}^0$ vertex ($\cos \theta_{\text{dir}}$) [24].

Further discrimination between signal and background categories is achieved by calculating weights for the remaining $\bar{D}^0 \pi^+ \pi^-$ candidates [25]. The weights are used by the

NeuroBayes neural network package [26] to maximise the separation between categories. A total of 15 variables are used in the network. They include the χ_{IP}^2 of the four candidate tracks, the χ_{IP}^2 , χ_{vertex}^2 , χ_{flight}^2 and $\cos\theta_{\text{dir}}$ of the \bar{D}^0 and $B_{(s)}^0$ candidates, and the $B_{(s)}^0$ candidate p_{T} . Variables describing the p_{T} asymmetry and track multiplicity in a 1.5 rad cone [4] around the $B_{(s)}^0$ candidate flight direction are also used. The input quantities to the neural network only depend weakly on the kinematics of the $B_{(s)}^0$ decay. A requirement on the network output is imposed that reduces the combinatorial background by an order of magnitude while retaining about 80 % of the signal. No bias is observed by using data driven selection requirements.

To improve the $B_{(s)}^0$ candidate invariant mass resolution, the four-momenta of the tracks from the \bar{D}^0 candidate are adjusted so that their combined invariant mass matches the world average value [3]. An additional B^0 mass constraint is applied in the calculation of the Dalitz plot coordinates, which are used in the determination of event-by-event efficiencies. A small fraction ($\sim 5\%$ within the mass range described below) of candidates with invariant masses far from the $B_{(s)}^0$ peak fail the mass constrained fit, and are removed from the analysis.

To remove a large potential background from $B^0 \rightarrow D^{*-}(2010)\pi^+$, candidates in the $\bar{D}^0\pi^+\pi^-$ sample are rejected if $m_{D\pi}-m_D$ (for either pion charge) lies within $\pm 2.5\text{ MeV}/c^2$ of the nominal $D^{*-}-\bar{D}^0$ mass difference [3]. Candidates in the $\bar{D}^0K^+K^-$ sample are also rejected if the invariant mass difference calculated under the pion mass hypothesis satisfies the same criterion. This removes 3.3 % of $\bar{D}^0K^+K^-$ candidates. Less than 1 % of $\bar{D}^0K^+K^-$ combinations are rejected by requiring that the pion from the \bar{D}^0 candidate together with the two kaons do not form an invariant mass in the range 1950–1975 MeV/c^2 , which removes potential background from $B_s^0 \rightarrow D_s^\mp K^\pm$ decays.

After all selection requirements are applied, less than 1 % of events with at least one candidate also contain a second candidate. Such multiple candidates are retained and treated the same as other candidates; the associated systematic uncertainty is negligible.

In addition to combinatorial background, candidates may be formed from misidentified or partially reconstructed $B_{(s)}^0$ decays, or from $B_{(s)}^0$ decays to identical final states but without intermediate charmed mesons (referred to below as charmless peaking background). Contributions from partially reconstructed decays are reduced by requiring the invariant mass of the $B_{(s)}^0$ candidate to be above 5150 MeV/c^2 . Sources of misidentified backgrounds are investigated using simulation. Most potential sources are found to have a broad invariant mass distribution, and are absorbed in the combinatorial background shape used in the fit described below. Backgrounds from $\bar{\Lambda}_b^0 \rightarrow \bar{D}^0\bar{p}K^+$ and $\bar{\Lambda}_b^0 \rightarrow \bar{D}^0\bar{p}\pi^+$ [27], $B^0 \rightarrow \bar{D}^0K^+\pi^-$ and $B_s^0 \rightarrow \bar{D}^0K^-\pi^+$ decays may, however, give contributions with distinctive shapes and therefore need to be included in the fit.

The contributions from charmless peaking background are investigated using candidates, reconstructed without the \bar{D}^0 mass constraint, in sideband regions around the \bar{D}^0 mass. The distributions are fitted with double Gaussian signal and linear background probability density functions (PDFs). Extrapolating to the D mass signal region, 773 ± 30 (126 ± 18) charmless background decays are expected in the $\bar{B}^0 \rightarrow \bar{D}^0\pi^+\pi^-$

($\bar{B}^0 \rightarrow \bar{D}^0 K^+ K^-$) distributions. No peaking background is observed in the B_s^0 region.

The signal yields are obtained from unbinned maximum likelihood fits to the $\bar{D}^0 \pi^+ \pi^-$ and $\bar{D}^0 K^+ K^-$ invariant mass distributions in the range 5150–5600 MeV/ c^2 . There are 14 214 $\bar{D}^0 \pi^+ \pi^-$ and 2990 $\bar{D}^0 K^+ K^-$ candidates. The $\bar{D}^0 \pi^+ \pi^-$ fit includes a double Gaussian shape for signal, together with an exponential component for partially reconstructed background, and a PDF for $\bar{\Lambda}_b^0 \rightarrow \bar{D}^0 X$ decays modelled using a non-parametric function obtained from simulation. The $\bar{D}^0 K^+ K^-$ fit includes a second double Gaussian component to account for the possible presence of both B^0 and B_s^0 decays, and peaking background PDFs for $\bar{\Lambda}_b^0 \rightarrow \bar{D}^0 \bar{p} K^+$, $B^0 \rightarrow \bar{D}^0 K^+ \pi^-$ and $B_s^0 \rightarrow \bar{D}^0 K^- \pi^+$, all modelled using non-parametric functions. The shape of the combinatorial background is essentially linear, but is multiplied by a function that accounts for the fact that candidates with high invariant masses are more likely to fail the $B_{(s)}^0$ mass constrained fit.

The result of the fit to $\bar{D}^0 \pi^+ \pi^-$ candidates is shown in Fig. 2. There are nine free parameters in this fit: the double Gaussian peak position, core width and fraction in the core, the linear slope of the combinatorial background and the exponential shape parameter of the partially reconstructed background, and the yields of the four categories. The relative width of the broader to the core Gaussian component is constrained within uncertainty to the value obtained in simulation. The fit yields 8060 ± 150 $B^0 \rightarrow \bar{D}^0 \pi^+ \pi^-$ decays, including charmless peaking background.

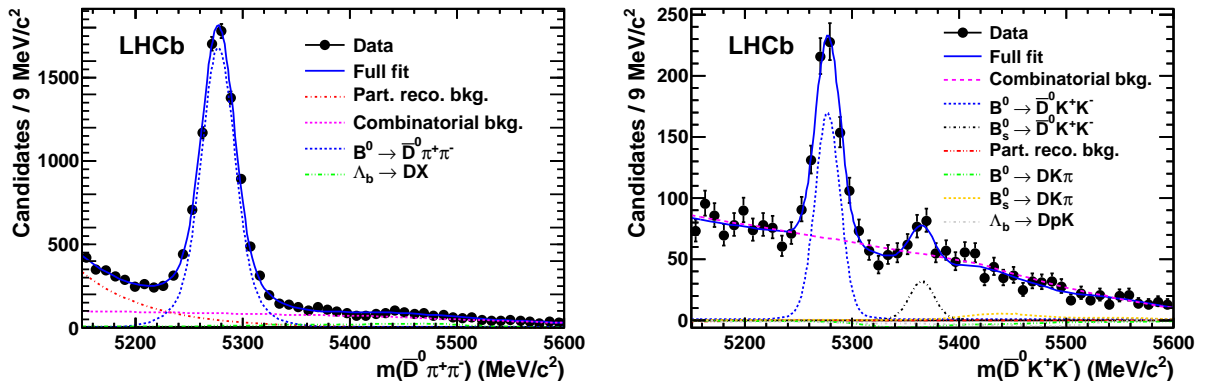


Figure 2: Fits to the $B_{(s)}^0$ candidate invariant mass distributions for the (left) $\bar{D}^0 \pi^+ \pi^-$ and (right) $\bar{D}^0 K^+ K^-$ samples. Data points are shown in black, the full fitted PDFs as solid blue lines and the components as detailed in the legends. Yields of the partially reconstructed and peaking backgrounds are all small for the $\bar{D}^0 K^+ K^-$ sample.

Since the fit to $\bar{D}^0 K^+ K^-$ candidates, shown in Fig. 2, has more components, additional constraints are imposed in order to improve the stability of the results. The parameters of the double Gaussian shapes are constrained to be identical for B^0 and B_s^0 signals, with an offset in their mean values fixed to the known B^0 – B_s^0 mass difference [3]. The slope of the combinatorial component is constrained to the value obtained in the fit to \bar{D}^0 mass sideband events. The exponential shape parameter is constrained to the value obtained

in the $\bar{D}^0\pi^+\pi^-$ fit. The fit yields 558 ± 49 $B^0 \rightarrow \bar{D}^0 K^+ K^-$ decays, including charmless peaking background, and 104 ± 29 $B_s^0 \rightarrow \bar{D}^0 K^+ K^-$ decays. All background yields are consistent with their expectations within uncertainties.

The ratio of branching fractions is obtained after subtracting the charmless peaking background, and applying event-by-event efficiencies as a function of the Dalitz plot position

$$\frac{\mathcal{B}(B^0 \rightarrow \bar{D}^0 K^+ K^-)}{\mathcal{B}(B^0 \rightarrow \bar{D}^0 \pi^+ \pi^-)} = R(B^0, B^0) = \frac{N^{\text{corr}}(\bar{D}^0 K^+ K^-) \left(1 - \frac{N^{\text{peak}}(\bar{D}^0 K^+ K^-)}{N(\bar{D}^0 K^+ K^-)}\right)}{N^{\text{corr}}(\bar{D}^0 \pi^+ \pi^-) \left(1 - \frac{N^{\text{peak}}(\bar{D}^0 \pi^+ \pi^-)}{N(\bar{D}^0 \pi^+ \pi^-)}\right)}, \quad (1)$$

where N is the yield obtained from the fit, N^{peak} is the charmless peaking background contribution, and the efficiency corrected yield $N^{\text{corr}} = \sum_i W_i / \epsilon_i^{\text{tot}}$. Here the index i runs over all candidates in the fit range, W_i is the signal weight for candidate i [25] from the fit shown in Fig. 2 and ϵ_i^{tot} is the efficiency for candidate i , which depends only on its Dalitz plot position. The statistical uncertainty on the branching fraction ratio incorporates the effects of the shape parameters that are allowed to vary in the fit, the dilution due to event weighting, and the charmless peaking background subtraction. Most potential systematic effects cancel in the ratio.

The PID efficiency is measured using a control sample of $D^{*-} \rightarrow \bar{D}^0 \pi^-$, $\bar{D}^0 \rightarrow K^+ \pi^-$ decays to obtain background-subtracted efficiency tables for kaons and pions as functions of their p and p_T [28]. The kinematic properties of the tracks in signal decays are obtained from simulation, allowing the PID efficiency for each event to be obtained from the tables taking into account the correlation between the p and p_T values of the two tracks. The other contributions to the efficiency (detector acceptance, selection criteria and trigger effects) are determined from simulation, and validated using data. All are found to be approximately constant across the Dalitz plane, apart from some modulations seen near the kinematic boundaries.

The Dalitz plot distributions obtained from the signal weights are shown in Fig. 3. The $B^0 \rightarrow \bar{D}^0 \pi^+ \pi^-$ distribution shows contributions from the $\rho^0(770)$ and $f_2(1270)$ resonances (upper diagonal edge of the Dalitz plot) and from the $D_2^{*-}(2460)$ state (horizontal band), as expected from previous studies of this decay [17, 18]. The $B^0 \rightarrow \bar{D}^0 K^+ K^-$ distribution shows a possible contribution from the $D_{s2}^{*-}(2573)$ resonance, together with an enhancement of events at low $K^+ K^-$ invariant mass (upper diagonal edge).

The branching fraction of the B_s^0 decay to $\bar{D}^0 K^+ K^-$ is measured relative to that of B^0 to the same final state. Due to the low yield in this decay, an event-by-event efficiency correction is not used. The ratio of branching fractions is instead determined as

$$\frac{\mathcal{B}(B_s^0 \rightarrow \bar{D}^0 K^+ K^-)}{\mathcal{B}(B^0 \rightarrow \bar{D}^0 K^+ K^-)} = R(B_s^0, B^0) = \left(\frac{f_s}{f_d}\right)^{-1} \frac{N(B_s^0 \rightarrow DKK)}{N(B^0 \rightarrow DKK) - N^{\text{peak}}(B^0 \rightarrow DKK)}. \quad (2)$$

The ratio of fragmentation fractions is $f_s/f_d = 0.267_{-0.020}^{+0.021}$ [29].

Systematic uncertainties are assigned to both branching fraction ratios due to the following sources. The variation of efficiency across the Dalitz plot may not be correctly

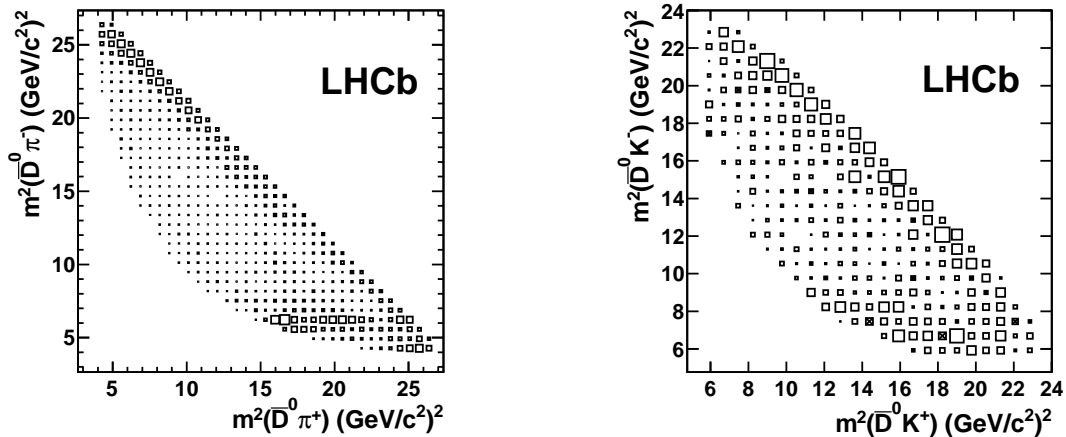


Figure 3: Dalitz plot distributions for (left) $B^0 \rightarrow \bar{D}^0 \pi^+ \pi^-$ and (right) $B^0 \rightarrow \bar{D}^0 K^+ K^-$ obtained from the signal weights. Note that these distributions contain contributions from charmless peaking backgrounds.

modelled in simulation. The difference, 6.7%, between the nominal result for $R(B^0, B^0)$ and that obtained using Dalitz plot averaged efficiencies is conservatively taken as an estimate of the associated systematic uncertainty. The fit model is varied by scaling the B_s^0/B^0 PDF width ratio to account for their different masses, removing components with small yields, adding components for potential background from $B_s^0 \rightarrow \bar{D}^{*0} \bar{K}^{*0}$ and $B_s^0 \rightarrow \bar{D}^{*0} K^+ K^-$, and varying the linear parameter of the combinatorial background PDF within uncertainties from the fit to the \bar{D}^0 sidebands used to estimate the charmless peaking background. Together these contribute 10.7% (19.9%) to $R(B^0, B^0)$ ($R(B_s^0, B^0)$). An uncertainty of 1.5% is assigned due to the charmless peaking background subtraction procedure. Possible biases in the determination of the fit parameters are investigated using MC pseudoexperiments, leading to 1.5% (3.4%) uncertainty on the $R(B^0, B^0)$ ($R(B_s^0, B^0)$).

In addition, the possible differences in the data/MC ratios of trigger and PID efficiencies between the two channels (both 2.0%) and the effect of the D_s^+ veto (1.7%) affect only $R(B^0, B^0)$. The uncertainty on the quantity f_s/f_d (7.9%) affects only $R(B_s^0, B^0)$. The total systematic uncertainties are obtained as the quadratic sums of all contributions.

A number of cross-checks are performed to test the stability of the result. The data sample is divided by dipole magnet polarity, data taking period and trigger category. Candidates were divided based upon the hardware trigger decision into three groups; events in which a particle from the signal decay created a large enough cluster in the calorimeter to fire the trigger, events that were triggered independently of the signal decay and those events that were triggered by both the signal decay and the rest of the event. The neural network and PID requirements are tightened and loosened. The PID efficiency is evaluated using the kinematic properties from $\bar{D}^0 \pi^+ \pi^-$ data instead of from simulation. The charmless peaking background contribution is determined from the upper and lower \bar{D}^0 mass sidebands separately. All give consistent results.

The significances of the signals are obtained from the changes in likelihood in fits to data with and without signal components, after accounting for systematic uncertainties and for charmless peaking background in $B^0 \rightarrow \bar{D}^0 K^+ K^-$ only. They are found to be 5.8σ and 3.8σ for $B^0 \rightarrow \bar{D}^0 K^+ K^-$ and $B_s^0 \rightarrow \bar{D}^0 K^+ K^-$ respectively.

In summary, the decay $B^0 \rightarrow \bar{D}^0 K^+ K^-$ has been observed for the first time, and its branching fraction relative to that of $B^0 \rightarrow \bar{D}^0 \pi^+ \pi^-$ is measured to be

$$\frac{\mathcal{B}(B^0 \rightarrow \bar{D}^0 K^+ K^-)}{\mathcal{B}(B^0 \rightarrow \bar{D}^0 \pi^+ \pi^-)} = 0.056 \pm 0.011 \pm 0.007,$$

where the first uncertainty is statistical and the second is systematic. Using the known value of $\mathcal{B}(B^0 \rightarrow \bar{D}^0 \pi^+ \pi^-) = (8.4 \pm 0.4 \pm 0.8) \times 10^{-4}$ [17], this gives

$$\mathcal{B}(B^0 \rightarrow \bar{D}^0 K^+ K^-) = (4.7 \pm 0.9 \pm 0.6 \pm 0.5) \times 10^{-5},$$

where the third uncertainty arises from $\mathcal{B}(B^0 \rightarrow \bar{D}^0 \pi^+ \pi^-)$. Evidence for the $B_s^0 \rightarrow \bar{D}^0 K^+ K^-$ decay has also been found, with relative branching fraction

$$\frac{\mathcal{B}(B_s^0 \rightarrow \bar{D}^0 K^+ K^-)}{\mathcal{B}(B^0 \rightarrow \bar{D}^0 K^+ K^-)} = 0.90 \pm 0.27 \pm 0.20.$$

A future study of the Dalitz plot distributions of these decays will provide insight into the dynamics of hadronic B decays. In addition, the $B_s^0 \rightarrow \bar{D}^0 K^+ K^-$ decay may be used to measure the CP violating phase γ .

Acknowledgements

We express our gratitude to our colleagues in the CERN accelerator departments for the excellent performance of the LHC. We thank the technical and administrative staff at CERN and at the LHCb institutes, and acknowledge support from the National Agencies: CAPES, CNPq, FAPERJ and FINEP (Brazil); CERN; NSFC (China); CNRS/IN2P3 (France); BMBF, DFG, HGF and MPG (Germany); SFI (Ireland); INFN (Italy); FOM and NWO (The Netherlands); SCSR (Poland); ANCS (Romania); MinES of Russia and Rosatom (Russia); MICINN, XuntaGal and GENCAT (Spain); SNSF and SER (Switzerland); NAS Ukraine (Ukraine); STFC (United Kingdom); NSF (USA). We also acknowledge the support received from the ERC under FP7 and the Region Auvergne.

References

- [1] N. Cabibbo, *Unitary symmetry and leptonic decays*, Phys. Rev. Lett. **10** (1963) 531.
- [2] M. Kobayashi and T. Maskawa, *CP violation in the renormalizable theory of weak interaction*, Prog. Theor. Phys. **49** (1973) 652.

- [3] Particle Data Group, K. Nakamura *et al.*, *Review of particle physics*, J. Phys. **G37** (2010) 075021.
- [4] LHCb collaboration, R. Aaij *et al.*, *Observation of CP violation in $B^\pm \rightarrow DK^\pm$ decays*, Phys. Lett. **B712** (2012) 203, arXiv:1203.3662.
- [5] M. Gronau and D. London, *How to determine all the angles of the unitarity triangle from $B^0 \rightarrow DK_s^0$ and $B_s^0 \rightarrow D\phi$* , Phys. Lett. **B253** (1991) 483.
- [6] M. Gronau *et al.*, *Using untagged $B^0 \rightarrow DK_s^0$ to determine γ* , Phys. Rev. **D69** (2004) 113003, arXiv:hep-ph/0402055.
- [7] M. Gronau, Y. Grossman, Z. Surujon, and J. Zupan, *Enhanced effects on extracting γ from untagged B^0 and B_s^0 decays*, Phys. Lett. **B649** (2007) 61, arXiv:hep-ph/0702011.
- [8] S. Nandi and D. London, *$B_s(\bar{B}_s) \rightarrow D_{CP}^0 K\bar{K}$: detecting and discriminating New Physics in B_s - \bar{B}_s mixing*, Phys. Rev. **D85** (2012) 114015, arXiv:1108.5769.
- [9] BaBar collaboration, B. Aubert *et al.*, *Measurement of the branching fractions of the rare decays $B^0 \rightarrow D_s^{(*)+}\pi^-$, $B^0 \rightarrow D_s^{(*)+}\rho^-$, and $B^0 \rightarrow D_s^{(*)-}K^{(*)+}$* , Phys. Rev. **D78** (2008) 032005, arXiv:0803.4296.
- [10] Belle collaboration, A. Das *et al.*, *Measurements of branching fractions for $B^0 \rightarrow D_s^+\pi^-$ and $\bar{B}^0 \rightarrow D_s^+K^-$* , Phys. Rev. **D82** (2010) 051103, arXiv:1007.4619.
- [11] Belle collaboration, A. Drutskoy *et al.*, *Observation of $B \rightarrow D^{(*)}K^-K^{0(*)}$ decays*, Phys. Lett. **B542** (2002) 171, arXiv:hep-ex/0207041.
- [12] BaBar collaboration, B. Aubert *et al.*, *Observation of tree-level B decays with $s\bar{s}$ production from gluon radiation.*, Phys. Rev. Lett. **100** (2008) 171803, arXiv:0707.1043.
- [13] Belle collaboration, J. Wiechczynski *et al.*, *Measurement of $B \rightarrow D_s^{(*)}K\pi$ branching fractions*, Phys. Rev. **D80** (2009) 052005, arXiv:0903.4956.
- [14] LHCb collaboration, A. A. Alves Jr. *et al.*, *The LHCb detector at the LHC*, JINST **3** (2008) S08005.
- [15] V. V. Gligorov, *A single track HLT1 trigger*, LHCb-PUB-2011-003.
- [16] V. V. Gligorov, C. Thomas, and M. Williams, *The HLT inclusive B triggers*, LHCb-PUB-2011-016.
- [17] Belle collaboration, A. Kuzmin *et al.*, *Study of $\bar{B}^0 \rightarrow D^0\pi^+\pi^-$ decays*, Phys. Rev. **D76** (2007) 012006, arXiv:hep-ex/0611054.

- [18] BaBar collaboration, P. del Amo Sanchez *et al.*, *Dalitz-plot analysis of $B^0 \rightarrow \bar{D}^0 \pi^+ \pi^-$* , [arXiv:1007.4464](#).
- [19] T. Sjöstrand, S. Mrenna, and P. Skands, *PYTHIA 6.4 physics and manual*, JHEP **05** (2006) 026, [arXiv:hep-ph/0603175](#).
- [20] I. Belyaev *et al.*, *Handling of the generation of primary events in GAUSS, the LHCb simulation framework*, Nuclear Science Symposium Conference Record (NSS/MIC) **IEEE** (2010) 1155.
- [21] D. J. Lange, *The EvtGen particle decay simulation package*, Nucl. Instrum. Meth. **A462** (2001) 152.
- [22] GEANT4 collaboration, J. Allison *et al.*, *Geant4 developments and applications*, IEEE Trans. Nucl. Sci. **53** (2006) 270; GEANT4 collaboration, S. Agostinelli *et al.*, *GEANT4: A simulation toolkit*, Nucl. Instrum. Meth. **A506** (2003) 250.
- [23] M. Clemencic *et al.*, *The LHCb simulation application, Gauss: design, evolution and experience*, J. Phys. : Conf. Ser. **331** (2011) 032023.
- [24] LHCb collaboration, R. Aaij *et al.*, *First observation of the decay $\bar{B}_s^0 \rightarrow D^0 K^{*0}$ and a measurement of the ratio of branching fractions $\frac{\mathcal{B}(\bar{B}_s^0 \rightarrow D^0 K^{*0})}{\mathcal{B}(B^0 \rightarrow D^0 \rho^0)}$* , Phys. Lett. **B706** (2011) 32, [arXiv:1110.3676](#).
- [25] M. Pivk and F. R. Le Diberder, *SPlot: A statistical tool to unfold data distributions*, Nucl. Instrum. Meth. **A555** (2005) 356, [arXiv:physics/0402083](#).
- [26] M. Feindt and U. Kerzel, *The NeuroBayes neural network package*, Nucl. Instrum. Meth. **A559** (2006) 190.
- [27] LHCb collaboration, *Studies of beauty baryons decaying to $D^0 p \pi^-$ and $D^0 p K^-$* , LHCb-CONF-2011-036.
- [28] LHCb collaboration, R. Aaij *et al.*, *Measurement of b-hadron branching fractions for two-body decays into charmless charged hadrons*, [arXiv:1206.2794](#), submitted to JHEP.
- [29] LHCb collaboration, R. Aaij *et al.*, *Measurement of b hadron production fractions in 7 TeV pp collisions*, Phys. Rev. **D85** (2012) 032008, [arXiv:1111.2357](#).